ChemPubSoc Europe

DOI: 10.1002/cphc.201900183

CHEMPHYSCHEM Articles

Special Issue

Systematic Experimental Study on Quantum Sieving of Hydrogen Isotopes in Metal-Amide-Imidazolate Frameworks with narrow 1-D Channels

Suvendu Sekhar Mondal,[a] Alex Kreuzer,[b] Karsten Behrens,[a] Gisela Schütz,[b] Hans-Jürgen Holdt,[a] and Michael Hirscher*[b]

Quantum sieving of hydrogen isotopes is experimentally studied in isostructural hexagonal metal-organic frameworks having 1-D channels, named IFP-1, −3, −4 and −7. Inside the channels, different molecules or atoms restrict the channel diameter periodically with apertures larger (4.2 Å for IFP-1, 3.1 Å for IFP-3) and smaller (2.1 Å for IFP-7, 1.7 Å for IFP-4) than the kinetic diameter of hydrogen isotopes. From a geometrical point of view, no gas should penetrate into IFP-7 and IFP-4, but due to the thermally induced flexibility, so-called gate-opening effect of the apertures, penetration becomes possible with increasing temperature. Thermal desorption spectroscopy (TDS) measurements with pure H_2 or D_2 have been applied to study isotope adsorption. Further TDS experiments after exposure to an equimolar H_2/D_2 mixture allow to determine directly the selectivity of isotope separation by quantum sieving. IFP-7 shows a very low selectivity not higher than $S=2$. The selectivity of the materials with the smallest pore aperture IFP-4 has a constant value of $S\approx2$ for different exposure times and pressures, which can be explained by the 1-D channel structure. Due to the relatively small cavities between the apertures of IFP-4 and IFP-7, molecules in the channels cannot pass each other, which leads to a single-file filling. Therefore, no time dependence is observed, since the quantum sieving effect occurs only at the outermost pore aperture, resulting in a low separation selectivity.

1. Introduction

Deuterium, a stable isotope of hydrogen, has been recognized as a potential energy source for nuclear fusion reactors and is widely used today in numerous industrial and scientific applications. It is challenging to satisfy the world demand, as deuterium makes up only 0.0156% of the naturally occurring hydrogen isotopes.[1] Moreover, its extraction from isotope mixtures is difficult as the isotopes possess the same size and chemical properties. The conventional techniques for H_2/D_2 separation, like cryogenic distillation, the Girdler Sulfide process, thermal diffusion, and centrifugation are highly energy consuming, and therefore expensive.[2] Furthermore, the selectivity of these techniques is less than 2.5.

Beenakker *et al.*[3] suggested that quantum sieving (QS) is one promising avenue to separate hydrogen isotopes efficiently. QS takes place when the difference between pore and molecular size becomes comparable to the de Broglie wavelength of molecular hydrogen, as heavier isotopes are confined more than lighter ones in the pore due to the difference in the zero point energy (ZPE). Thus, the lower the temperature in the confined system, the stronger the diffusion coefficients of the isotopes will differ inside the porous material, resulting in the separation of the isotopes.[4] Therefore, in this kinetic isotope QS, the aperture size plays an important role for determining the diffusion kinetics and thereby overall separation. This has initiated an ongoing effort to elucidate this phenomenon and to find more effective ultramicroporous materials.[5–14]

By now, only a few porous materials like carbons, zeolites, and metal-organic frameworks (MOFs)[15–19] have been experimentally studied. Owing to their crystallinity with well-defined pore size, nanoporous MOFs are excellent candidates for applications in hydrogen isotope sieving. An experimental study on covalent organic frameworks (COFs) and zeolitic imidazolate frameworks (ZIFs) with different apertures[16] showed an optimum pore aperture for quantum sieving lies between 3 Å and 3.4 Å.

Few of us have previously reported Zn based isostructural Imidazolate Framework Potsdam (IFP) that was formed under solvothermal conditions in *N,N'*-dimethylformamide (DMF)[20–23]. The imidazolate chelate ligand, 2-substituted imidazolate-4-amide-5- imidate linker [2(a–d)] (R = Me, Br, Et and OMe) was generated in situ by partial hydrolysis of 4,5- dicyano-2-substututed imidazole [1(a–d)] under solvothermal conditions

[a] Dr. S. S. Mondal, Dr. K. Behrens, Prof. H.-J. Holdt
Institut für Chemie, Anorganische Chemie
Universität Potsdam
Karl-Liebknecht-Straße 24–25, 14476 Potsdam, Germany
[b] A. Kreuzer, Prof. Dr. G. Schütz, Dr. M. Hirscher
Modern Magnetic Systems
Max Planck Institute for Intelligent Systems
Heisenbergstr. 3, 70569 Stuttgart
E-mail: hirscher@is.mpg.de

Supporting information for this article is available on the WWW under https://doi.org/10.1002/cphc.201900183

An invited contribution to a Special Issue on Hydrogen Energy

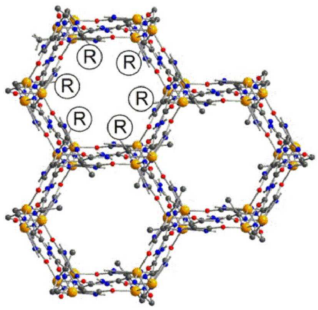

R	Accessible pore aperture [Å]
IFP-1 Me	4.2
IFP-3 Br	3.1
IFP-7 OMe	2.1
IFP-4 Et	1.7

Figure 1. Schematic presentation of 1-D hexagonal channels IFP structures, showing substituent (at right) and corresponding pore aperture.

and in the presence of zinc nitrate hydrate salt (Scheme S1 at ESI). The Zn^{2+} ion is pentacoordinated by donor atoms of three ligands to form a distorted environment with a trigonal-bipyramidal geometry.[20] The structure of the IFPs have been previously resolved by X-ray crystallographic analyses and confirmed by IR and NMR spectroscopy.[21] In situ functionalized ligand linked with Zn^{2+} ions and form the neutral microporous imidazolate MOF with 1-D hexagonal channels (Figure 1). Zn^{2+} ions at IFP structure and bridging ligands act as 3-connected topological species forming a net with a uninodal topology, named *etb*. The functional groups of C2 position of the linker protrude into the open channels, tuning the pore aperture (4.2−1.7 Å), polarity and functionality of the channel walls (Figure 1). Furthermore the specific surface area of IFP is depending on the substituent. The specific surface areas were determined by Debatin *et al.*[21] for IFP-1, −3 and −4 and by Mondal *et al.*[22] for IFP-7 based on the Brunauer-Emmett-Teller (BET) model measuring adsorption isotherms of N_2 at 77 K. Assuming a rigid channel structure, molecules with a kinetic diameter of 3.6 Å can not penetrate into the IFP-3, −7 and −4. Adsorption measurements with N_2 at 77 K have shown a decrease of specific surface area with the channel diameter as follows: 802 $m^2 g^{-1}$ (IFP-1), 324 $m^2 g^{-1}$ (IFP-3), 3 $m^2 g^{-1}$ (IFP-7) and 5 $m^2 g^{-1}$ (IFP-4). The low value of the BET surface area of 3 and 5 $m^2 g^{-1}$ for the materials with the smallest pore aperture leads to the conclusion that only the outer surface of the material was populated by N_2 molecules. For IFP materials with smaller pore aperture than the kinetic diameter of nitrogen, the thermally activated flexibility of the ethyl groups allows a penetration of N_2 into the IFP material. Hydrogen isotopes with smaller kinetic diameter than N_2 are therefore expected to enter the IFP structure at lower temperatures. Therefore, the isostructural IFP series with flexible apertures are used to further elucidate the influence of the aperture size on quantum sieving of hydrogen isotopes. The selectivity was experimentally determined by thermal desorption spectroscopy (TDS) after exposure to H_2/D_2 mixtures at several temperatures and for different times.

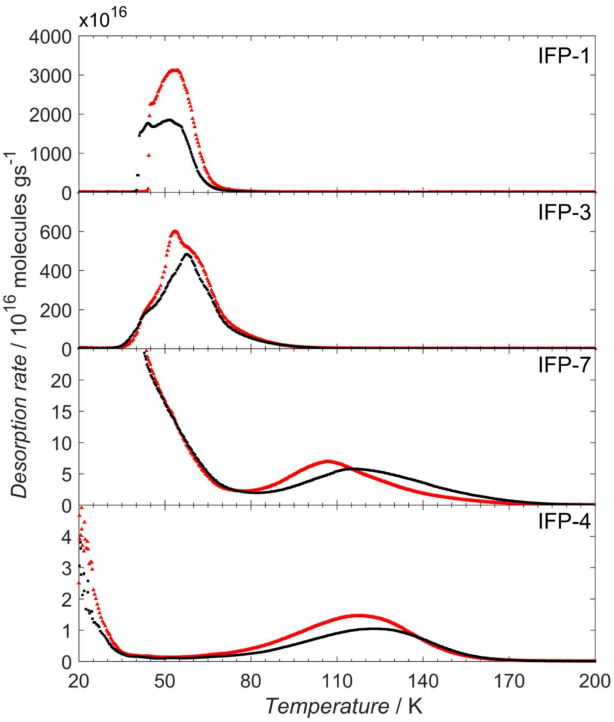

Figure 2. 10 mbar of pure H_2 (in black) or D_2 (in red) have been exposed to the IFP-1, -3, -4 and -7 samples at room temperature of 298 K and cooled to 20 K under gas atmosphere. (Heating rate: 0.1 $K s^{-1}$).

2. Results and Discussion

Hydrogen isotope adsorption of the IFP samples was studied with TDS. The IFP have been exposed to pure H_2 or D_2 gas separately at 10 mbar at room temperature for two hours and then cooled under hydrogen isotope atmosphere. After cooling down to 20 K the remaining gas was pumped out and TDS was performed heating the material with a constant heating rate of 0.1 $K s^{-1}$ and measuring the temperature dependent desorption rate.

The desorption spectra of the different IFPs measured separately with pure H_2 or D_2 gas are shown in figure 2. The desorption rate of pure D_2 (red line) always exceeds the one of pure H_2 (black line), due to the slightly higher heat of adsorption of the heavier isotope. For IFP-1 and IFP-3, the maximal desorption rate is reached at lower temperatures about 60 K and ends at 80 K and 100 K, whereas for IFP-7 and IFP-4 the maximum appears above 100 K desorption temperature and ends at about 180 K. The amount of absorbed gas is different for each IFP material. IFP-1 absorbs about five times more hydrogen isotope molecules than IFP-3. The same holds for IFP-7 compared to IFP-4. Furthermore IFP-1 and IFP-3 absorb up to three orders of magnitude more hydrogen isotopes compared to IFP-7 and IFP-4. Since IFP-1 and −3 have the largest aperture diameters, they absorb clearly the highest amount of isotopes and show a steep increase of the desorption rate at low temperatures. The decreasing total amount of adsorbed hydrogen isotope molecules is consistent

with the decreasing specific surface areas of IFP-1 to IFP-7 analysed by BET measurements.[21,22]

The TDS spectra (Figure 2) of the MOF materials IFP-1 and IFP-3 with a pore diameter larger than the kinetic diameter of H_2 or D_2 show maxima with some substructure, i.e., shoulders, indicating that they consist of several maxima, which are caused by different adsorption sites, and furthermore, the maximum desorption temperature for H_2 and D_2 is similar within the accuracy of measurement. In contrast, the MOF materials with smaller pore diameter, IFP-4 and IFP-7, exhibit a single maximum and the maximum desorption temperatures of the H_2 spectra are shifted to higher temperatures compared to the D_2 spectra. In this case, the desorption is governed by the penetration through the small aperture and does not allow to observe different adsorption sites inside the pores. The desorption temperature is related to the diffusion of the isotopes through the gates and owing to this confinement the heavier molecule diffuses faster,[3] i.e., D_2 is released at lower temperatures. Additionally, for IFP-4 and IFP-7 a high desorption signal is visible at low temperatures which can be ascribed to the release of gas condensed in inter-particle voids of the powder. This signal occurs as well for IFP-1 and IFP-3 with comparable magnitude, but is not visible in figure 2 due to the difference of two orders of magnitude in the y-axis scale.

The capability for hydrogen isotope separation (quantum sieving) of the different MOFs has been investigated directly by exposure of the IFP material to an equimolar H_2/D_2 gas mixture for different exposure times and pressures. The exposure temperature for the different samples has been chosen by two criteria: *i*) the exposure temperature should be below the major desorption maximum *ii*) the exposure temperature should be well above the temperature where gas can penetrate into the pores, i.e., above the gate-opening temperature. Therefore, for IFP-1 and IFP-3, which have the largest pore aperture and the lowest desorption temperatures, the equimolar H_2/D_2 gas mixture was loaded at 30 K. Whereas for IFP-7 and IFP-4, 77 K was chosen as exposure temperature, since gas started to penetrate into the structure at 40 and 50 K, respectively, and the main desorption starts at 80 K. For all four IFPs, the total amount of absorbed H_2 and D_2 gas measured by TDS together with the respective selectivity are given in Tables 1 and 2 for different exposure times and pressures (corresponding TDS spectra see ESI).

IFP-1 shows no significant dependence of the total absorbed gas amount H_2+D_2 neither on the exposure time nor on the exposure pressure within the experimental accuracy (Table 1), since this IFP material with largest pore aperture is already loaded in a short time at low pressures. For IFP-3 the total absorbed amount increases slightly with exposure time, which implies only a small diffusion limitation. Thus for IFP-1 and IFP-3 practically no diffusion limitation occurs. Since quantum sieving is based on the diffusion limitation of the lighter isotope, the observed sieving with IFP-1 and IFP-3 is mainly caused by Chemical Affinity Quantum Sieving (CAQS). D_2 with lower zero point energy has stronger chemical affinity to the inner surface than H_2 and, therefore, is predominantly adsorbed on the pore walls.[24] The pore aperture of IFP-3 lies within the range of optimum pore aperture determined to be between 3.0 Å and 3.4 Å by Oh *et al.* .[16] However, the selectivity of IFP-3 is rather low beneath S = 3. Therefore no significant quantum sieving can be observed with IFP-1 and IFP-3.

The MOF materials IFP-4 and IFP-7 with smaller apertures than the kinetic diameter of hydrogen isotopes show an increase of the total absorbed gas amount with exposure time (Table 2). Moreover, with the small aperture the loading

Table 1. Summary of TDS results for IFP-1 and IFP-3, with pore apertures larger than the kinetic diameter of hydrogen isotopes. Amount of absorbed H_2 and D_2 molecules per gram (area under the TDS spectrum) and selectivity, S, after exposure at T_{ex} = 30 K to an equimolar gas mixture for different exposure times, t_{ex}, for p_{ex} = 10 mbar. Additionally, for IFP-1 the pressure dependence is shown for t_{ex} = 10 min.

T_{ex} = 30 K p_{ex} = 10 mbar	10 min	30 min	60 min
IFP-1 (4.2 Å)			
H_2 [10^{20} molecules/g]	2.54	2.24	2.21
D_2 [10^{20} molecules/g]	4.30	4.32	4.34
H_2+D_2 [10^{20} molecules/g]	6.84	6.56	6.55
S	1.69	1.93	1.97
IFP-3 (3.1 Å)			
H_2 [10^{20} molecules/g]	0.67	0.81	1.06
D_2 [10^{20} molecules/g]	1.60	2.23	2.42
H_2+D_2 [10^{20} molecules/g]	2.27	3.04	3.48
S	2.41	2.77	2.29
T_{ex} = 30 K t_{ex} = 10 min	10 mbar	30 mbar	60 mbar
IFP-1 (4.2 Å)			
H_2 [10^{20} molecules/g]	2.54	2.25	2.31
D_2 [10^{20} molecules/g]	4.30	4.98	5.26
H_2+D_2 [10^{20} molecules/g]	6.84	7.22	7.52
S	1.69	2.22	2.28

Table 2. Summary of TDS results for IFP-7 and IFP-4, with smaller pore apertures than the kinetic diameter of hydrogen molecules, after equimolar mixture exposure at T_{ex} = 77 K. Exposure time and pressure dependence of amount of absorbed H_2 and D_2 and selectivity for p_{ex} = 10 mbar and t_{ex} = 60 min, respectively.

T_{ex} = 77 K p_{ex} = 10 mbar	10 min	60 min	120 min
IFP-7 (2.1 Å)			
H_2 [10^{18} molecules/g]	0.92	2.05	2.80
D_2 [10^{18} molecules/g]	1.01	2.80	4.09
H_2+D_2 [10^{18} molecules/g]	1.93	4.85	6.89
S	1.10	1.37	1.46
IFP-4 (1.7 Å)			
H_2 [10^{18} molecules/g]	0.14	0.58	0.95
D_2 [10^{18} molecules/g]	0.28	1.22	1.95
H_2+D_2 [10^{18} molecules/g]	0.42	1.80	2.89
S	1.97	2.10	2.05
T_{ex} = 77 K t_{ex} = 60 min	10 mbar	30 mbar	60 mbar
IFP-7 (2.1 Å)			
H_2 [10^{18} molecules/g]	2.05	5.44	9.86
D_2 [10^{18} molecules/g]	2.80	8.24	15.28
H_2+D_2 [10^{18} molecules/g]	4.85	13.68	25.14
S	1.37	1.51	1.55
IFP-4 (1.7 Å)			
H_2 [10^{18} molecules/g]	0.58	1.18	1.91
D_2 [10^{18} molecules/g]	1.22	2.56	4.20
H_2+D_2 [10^{18} molecules/g]	1.80	3.74	6.10
S	2.10	2.16	2.20

procedure is much slower compared to IFP-1 and IFP-3 materials resulting in time dependence of the total absorbed amount within longer timescale of minutes or hours. Regarding the exposure pressure IFP-4 and IFP-7 show a clear dependence of the total absorbed gas amount on exposure pressure. The observed dependence on exposure time and pressure reveals that the diffusion is hindered and slow.

However, the selectivity of IFP-7 is rather low, below $S=2$, and IFP-4 shows a constant selectivity of about $S=2$ with exposure time and pressure. Figure 3 shows TDS desorption

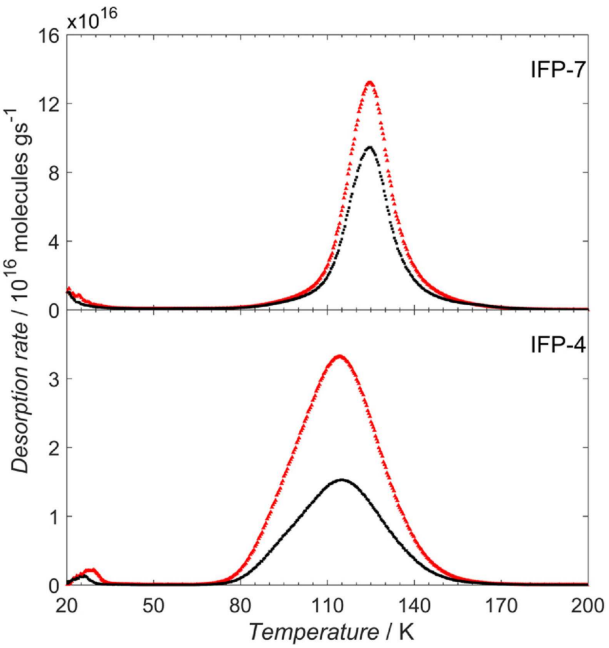

Figure 3. 10 mbar of an equimolar mixture of H_2 (in black) and D_2 (in red) have been exposed in the IFP-4 and -7 samples at 77 K for 60 min. (Heating rate 0.1 Ks^{-1}).

spectra of IFP-4 and IFP-7 exposed to an equimolar mixture at 10 mbar at 77 K for 60 min.

In case of the isotope mixture, the maximum desorption rate occurs at identical temperatures for H_2 and D_2, whereas the maximum desorption of pure gas in Figure 2 is located at lower temperatures for D_2 than for H_2, as expected from lower zero-point energy of the heavier isotope, and therefore, faster D_2 diffusion in the confinement.[3] The simultaneous desorption of H_2 and D_2 after mixture exposure is reasonable due to the single-file filling of hydrogen isotopes within the channel structure of small pores inside the material, which does not enable an exchange of hydrogen and deuterium molecules within those isotope sequences. Therefore, after isotope mixture exposure, due to the single-file filling, the diffusion of the isotopes is coupled and not independent. Additionally, for IFP-4 TDS measurements applying different heating rates have been performed after pure gas and mixture loadings. The desorption energy, which in this case of very small apertures, is dominated by penetration through the gate, has been evaluated applying the Kissinger method. Within the experimental uncertainty, the desorption energies are very similar, for pure H_2 and D_2 as well as H_2/D_2 mixture exposure, and about 7 $kJ\,mol^{-1}$ (for details see ESI). In summary, for IFP-7 and IFP-4 the single-file filling of isotopes into the one-dimensional channels is leading to a constant selectivity with exposure time and pressure, since quantum sieving takes only place at the outermost pore aperture.

Recently, MOFs and COFs with apertures smaller than the kinetic diameter of hydrogen molecules showing a gate opening or flexibility have been studied for quantum sieving. Teufel *et al.*[15] obtained a much higher selectivity of 7.5 by quantum sieving experiments on the framework of Cl-MFU-4, consisting of a structure with a combination of large and small pores. In this case, the small aperture and pore followed by a large pore allows a mixing of the isotope molecules in the large pores, and therefore, successive quantum sieving is occurring by further penetration into the pore structure. Another promising alternative for QS was presented by Oh *et al.*[18] using COFs including incorporated pyridine molecules, which are reducing the channel width and act as gates. Already at low temperatures beneath 30 K cryogenic flexibility enables gas penetration and quantum sieving reaching a selectivity of about 10 at a pressure of 26 mbar. Again, the alternating structure of narrow gates and channel sections with large volumes enable exchange and multiple quantum sieving.

3. Conclusions

In conclusion, the adsorption and quantum sieving of hydrogen isotopes H_2 and D_2 have been studied with IFPs, whose aperture diameters are crucial for their adsorption and isotope separation behaviour. The pore apertures of IFP-1 with 4.2 Å and IFP-3 with 3.1 Å are minimally larger than the kinetic diameter of hydrogen isotopes of 2.89 Å and are therefore suitable for quantum sieving. A comparison of IFP-1 and IFP-3 measured at 10 mbar and 30 K shows, that IFP-3 with the smaller pore aperture has the highest selectivity about $S=2.5$.

The pore apertures of IFP-7 with 2.1 Å and IFP-4 with 1.7 Å only allow adsorption of hydrogen isotopes due to a temperature dependent, dynamic gate opening, resulting in higher temperatures of the desorption spectra. Additionally, small apertures lead to slower diffusion of the isotope out of the IFP. The material with the smallest pore aperture, IFP-4, is showing a constant selectivity of $S\approx 2$ independent of pressure and longer exposure time. Since the small pore volumes prevent passing of hydrogen isotopes within the one dimensional channel structure, quantum sieving only occurs at the outermost pore aperture. Therefore, ultra-microporous materials with narrow 1-D channels lead to a poor selectivity for quantum sieving. This important result yields directly a structural design recipe for effective quantum sieving and achieving high selectivity. Two essential structural properties are required: *i)* small apertures for quantum sieving and *ii)* a successive sequence of apertures and large pore volumes, which then allow exchange of the isotope

molecules in the material and multiple quantum sieving at each aperture.

Experimental Section

The framework materials IFP-1, -3, -4 and -7 were synthesized according to the published procedures.[20-22] For general synthesis, 50 mg of the linker precursor and an equimolar amount of zinc nitrate hydrates (Scheme S1) were dissolved in DMF and placed in a in a sealed tube. The tube was closed and the mixture was heated up to 120 °C for 48–72 h and then cooled to room temperature. Crystalline IFP materials were filtrated, and washed with DMF and water.

Thermal desorption spectroscopy (TDS) experiments were performed in a homemade device[25] with a sample mass of about 3 mg of IFP powder. The high vacuum (HV) chamber contains the sample holder that is screwed tightly to a Cu block, which is surrounded by a resistive heater. This Cu block is connected to a cold finger of a flowing helium cryostat, which allows cooling below 20 K. The IFPs powder were activated at 423 K under vacuum for several hours. After exposure of the sample to H_2, D_2 or an equimolar isotope mixture at different temperatures, pressures and times, the remaining non-adsorbed gas is pumped out. The adsorbed gas is desorbed in vacuum by heating the sample with a constant heating rate. The desorption spectrum represents a fingerprint of the adsorbed state, where the area under the spectrum is proportional to the number of adsorbed molecules and the desorption temperature is proportional to the adsorption strength. In case of confinement in small pores the desorption temperature also reveals the diffusion of molecules out of the pores.

Acknowledgements

The authors like to thank Dr. Ingrid Zaiser for the elaborate TDS measurements and many discussions. This work is financially supported by the German Research Foundation (SPP 1362 "Porous Metal-Organic Frameworks," HO 1706/7-1and HO 1706/7-2).

Conflict of Interest

The authors declare no conflict of interest.

Keywords: gas adsorption · hydrogen isotopes · isotope separation · metal-organic frameworks · quantum sieving

[1] N. N. Greenwood, A. Earnshaw, *Chemistry of the Elements*, Elsevier Butterworth–Heinemann, Amsterdam/Heidelberg **2005**.
[2] H. K. Rae, in *Separation of Hydrogen Isotopes*, American Chemical Society, **1978**, pp. 1–26
[3] J. J. M. Beenakker, V. D. Borman, S. Y. Krylov, *Chem. Phys. Lett.* **1995**, *232*, 379–382.
[4] a) T. X. Nguyen, H. Jobic, S. K. Bhatia, *Phys. Rev. Lett.* **2010**, *105*, 085901. b) J. J. M. Beenakker, S. Y. Krylov, *J. Chem. Phys.* **1997**, *107*, 4015–4023.
[5] P. Kowalczyk, P. A. Gauden, A. P. Terzyk, S. Furmaniak, *Phys. Chem. Chem. Phys.* **2011**, *13*, 9824–9830.
[6] A. V. A. Kumar, S. K. Bhatia, *Phys. Rev. Lett.* **2005**, *95*, 245901.
[7] H. Tanaka, D. Noguchi, A. Yuzawa, T. Kodaira, H. Kanoh, K. Kaneko, *J. Low Temp. Phys.* **2009**, *157*, 352–373.
[8] P. Kowalczyk, P. A. Gauden, A. P. Terzyk, S. K. Bhatia, *Langmuir* **2007**, *23*, 3666–3672.
[9] X. B. Zhao, S. Villar-Rodil, A. J. Fletcher, K. M. Thomas, *J. Phys. Chem. B* **2006**, *110*, 9947–9955.
[10] J. K. Johnson, S. R. Challa, D. S. Sholl, *J. Chem. Phys.* **2002**, *116*, 814–824.
[11] G. Garberoglio, *Eur. Phys. J. D* **2009**, *51*, 185–191.
[12] P. Kowalczyk, P. A. Gauden, A. P. Terzyk, S. Furmaniak, *J. Phys. Condens. Matter* **2009**, *21*, 144210.
[13] Y. Wang, S. K. Bhatia, *J. Phys. Chem. C* **2009**, *113*, 14953–14962.
[14] H. Tanaka, H. Kanoh, M. Yudasaka, S. Lijima, K. Kaneko, *J. Am. Chem. Soc.* **2005**, *127*, 7511–7516.
[15] J. Teufel, H. Oh, M. Hirscher, M. Wahiduzzaman, L. Zhechkov, A. Kuc, T. Heine, D. Denysenko, D. Volkmer, *Adv. Mater.* **2013**, *25*, 635–639.
[16] H. Oh, K. S. Park, S. B. Kalidindi, R. A. Fischer, M. Hirscher, *J. Mater. Chem. A* **2013**, *1*, 3244–3248.
[17] H. Oh, I. Savchenko, A. Mavrandonakis, T. Heine, M. Hirscher, *ACS Nano* **2014**, *8*, 761–770.
[18] H. Oh, S. B. Kalidindi, Y. Um, S. Bureekaew, R. Schmid, R. A. Fischer, M. Hirscher, *Angew. Chem. Int. Ed.* **2013**, *52*, 13219–13222; *Angew. Chem.* **2013**, *125*, 13461–13464.
[19] I. Savchenko, A. Mavrandonakis, T. Heine, H. Oh, J. Teufel, M. Hirscher, *Microporous Mesoporous Mater.* **2015**, *216*, 133–137.
[20] F. Debatin, A. Thomas, A. Kelling, N. Hedin, Z. Bacsik, I. Senkovska, S. Kaskel, M. Junginger, H. Müller, U. Schilde, C. Jäger, A. Friedrich, H.-J. Holdt, *Angew. Chem. Int. Ed.* **2010**, *49*, 1258–1262; *Angew. Chem.* **2010**, *122*, 1280–1284.
[21] F. Debatin, K. Behrens, J. Weber, I. A. Baburin, A. Thomas, J. Schmidt, I. Senkovska, S. Kaskel, A. Kelling, N. Hedin, Z. Bacsik, S. Leoni, G. Seifert, C. Jäger, C. Günter, U. Schilde, A. Friedrich, H.-J. Holdt, *Chem. Eur. J.* **2012**, *18*, 11630–11640.
[22] S. S. Mondal, A. Bhunia, I. A. Baburin, C. Jäger, A. Kelling, U. Schilde, G. Seifert, C. Janiak, H.-J. Holdt, *Chem. Commun.* **2013**, *49*, 7599–7601.
[23] S. S. Mondal, *Design of isostructural metal-imidazolate frameworks: application for gas storage*, Faculty of Science, University of Potsdam, Potsdam, **2014**.
[24] H. Jiao, A. J. Du, M. Hankel, S. C. Smith, *Phys. Chem. Chem. Phys.* **2013**, *15*, 4832-4843.
[25] B. Panella, M. Hirscher, B. Ludescher, *Microporous Mesoporous Mater.* **2007**, *103*, 230–234.

Manuscript received: February 23, 2019
Revised manuscript received: April 23, 2019
Accepted manuscript online: April 24, 2019
Version of record online: May 2, 2019